

Diffuse Light in Galaxy Clusters

Magda Arnaboldi¹ and Ortwin Gerhard²

¹ European Southern Observatory, Karl Schwarzschild-Str 2, 85748 Garching, Germany
email: marnabol@eso.org

²Max Planck Institute for Extraterrestrial Physics, Giessenbachstrasse, 85748 Garching, Germany
email: gerhard@mpe.mpg.de

Abstract. Diffuse intracluster light (ICL) has now been observed in nearby and in intermediate redshift clusters. Individual intracluster stars have been detected in the Virgo and Coma clusters and the first color-magnitude diagram and velocity measurements have been obtained. Recent studies show that the ICL contains of the order of 10% and perhaps up to 30% of the stellar mass in the cluster, but in the cores of some dense and rich clusters like Coma, the local ICL fraction can be high as 40%-50%. What can we learn from the ICL about the formation of galaxy clusters and the evolution of cluster galaxies? How and when did the ICL form? What is the connection to the central brightest cluster galaxy? Cosmological N-body and hydrodynamical simulations are beginning to make predictions for the kinematics and origin of the ICL. The ICL traces the evolution of baryonic substructures in dense environments and can thus be used to constrain some aspects of cosmological simulations that are most uncertain, such as the modeling of star formation and the mass distribution of the baryonic component in galaxies.

Keywords. (cosmology:) large-scale structure of universe; galaxies: clusters: general; galaxies: evolution; galaxies: interactions; galaxies: structure; galaxies: kinematics and dynamics; galaxies: star clusters; (ISM:) planetary nebulae: general

1. Introduction

The Joint Discussion dedicated to the study of diffuse light in clusters took place on the 6th and 7th of August, 2009 during the XXVIIth IAU General Assembly in Rio de Janeiro. It was the first scientific meeting on this subject. This Joint Discussion provided a forum to confront observational evidence and theoretical predictions, and to identify future directions for understanding the origin and implications of this new component of galaxy clusters.

The Joint Discussion included four main sessions covering the distribution of diffuse light in clusters and groups, the kinematics of intracluster stars, the intracluster stellar populations, and the predictions of cosmological simulations for the evolution of galaxies in clusters and groups, and for the formation of the intracluster light. 14 invited plus 10 oral talks, and 14 poster papers contributed to an intense scientific exchange and set the stage for a lively scientific discussion, which concluded the workshop.

In what follows, we provide a brief summary and some selected references for the talks in the four sessions, and end with a summary of the discussion which took place on August 7th, 2009.



Figure 1. This deep image of the Virgo Cluster obtained by Chris Mihos and colleagues using the Burrell Schmidt telescope shows the diffuse light between the galaxies belonging to the cluster. North is up, east to the left. The dark spots indicate where bright foreground stars were removed from the image. M87 is the largest galaxy in the picture (lower left). From ESO PR19/2009, based on Mihos et al. (2005).

2. Distribution of diffuse light in cluster and groups

2.1. Clusters at $z = 0$

2.1.1. Diffuse light in the Virgo cluster - C. Mihos

Thanks to the specially adapted Burrell Schmidt telescope, the study of intracluster light in the Virgo cluster reached for the first time a photometric accuracy of significantly less than 1% of night sky emission over an area of many square degrees. Deep V ($\mu_V = 28.5 \text{ mag/arcsec}^2$) and B band ($\mu_B = 29.0 \text{ mag/arcsec}^2$) photometry with calibrated, quantitative photometric solutions and a well understood error model were obtained. This work has revealed faint surface brightness features over a multitude of angular scales, from narrow streams to extended diffuse halos. The B-V colour of the ICL is similar to that in the outer halos of ellipticals, except for some streamers, and there is a rough correlation with the spatial distribution of intracluster planetary nebulae. References: Mihos et al. (2005, 2009).

2.1.2. Diffuse light in the Coma cluster - C. Adami

Diffuse light in the Coma cluster is documented since the work of Zwicky in 1951. Photographic photometry in the 1970s revealed a large elongated diffuse component in the core of the cluster, around the two BCG galaxies. Several small-scale streamers and plumes were discovered in the 1990s with CCD photometry. The CFHT multi-color Coma survey shows that the diffuse light is found either in the centre of the Coma cluster or along the in-fall directions towards nearby large scale structures. The diffuse light in the cluster core was found to be distributed on different scales, as quantified by a wavelet analysis. References: Thuan & Kormendy (1977), Adami et al. (2005a, 2005b).

2.1.3. *Testing dark matter with the “star pile” in Abell 545: the faintest cD or the brightest ICL? - R. Salinas*

The study of surface brightness distribution of the star pile in Abell 545 shows that it can be described as the halo of a cD without the high surface brightness central galaxy. The light distribution in Abell 545 can thus be considered as independent evidence for intracluster light as a separate stellar component from the BCG halo. The spectroscopic follow-up shows that its spectrum is consistent with that of an old stellar population. References: Salinas et al. (2007).

2.2. *Groups at $z=0$: compact and fossil groups*

2.2.1. *Diffuse light and intra-group star-forming regions in compact groups of galaxies - C. Mendes de Oliveira*

Compact groups are high density regions in the universe where the morphology of both the stars and the HI gas in galaxies is often disturbed, providing evidence for on-going interactions. An evolutionary sequence for compact groups can be traced by the fraction of light in the diffuse component on the group scale, the intragroup light (IGL), which increases with the degree of interactions, reaching up to 30-40% in groups with many ongoing interactions. Groups with the highest fraction of IGL light are also those with the highest fraction of early type galaxies. The colour of the IGL in most cases is similar to the colours in the outskirts of the member galaxies. Star formation occurs in the intragroup medium when the compact group contains stripped HI and is in an intermediate to advanced stage of interaction. References: Da Rocha et al. (2008), de Mello et al. (2008), Torres-Flores et al. (2009).

2.2.2. *Wavelet analysis of diffuse intra-group optical light in compact groups of galaxies - C. Da Rocha*

The wavelet analysis of diffuse optical intra-group light in compact groups of galaxies can provide reliable measurements of the intragroup light on different scales. The diffuse light distributions in HCG 79 and HCG 51 are illustrated as prototype cases. References: Da Rocha et al. (2008).

2.3. *Clusters at $z=0.3$*

2.3.1. *Intracluster light in moderate redshift clusters - J.J. Feldmeier*

The review of photometric measurements of ICL fractions in clusters highlights the challenges posed by such measurements and their intrinsic limitations. The ICL is difficult to measure, being at best at the level of 1% of the night sky. Critical steps in the data reduction are the sky subtraction and flat fielding, which have to be precise to 0.1%. Severe obstacles are the effects of the large scale PSF and scattered light, and the separation of ICL from BCGs, cD halos and other galaxies. Fractions of the ICL are determined from photometric measurements, integrating the light outside the assumed outer radii of individual galaxies over the region confined within an isophote with surface brightness threshold defined by the depth of the observations. Such measurements for the ICL fractions are in the range from 10 to 45% - ICL is common in galaxy clusters. References: Feldmeier et al. (2004a), Gonzalez et al. (2007), Krick and Bernstein (2007).

2.3.2. *Statistical properties of the intracluster light at $z=0.25$ - S. Zibetti*

To quantify the amount of ICL and determine trends with cluster properties, key issues are statistics and depth. These can be addressed by stacking many shallow images, combining them into deeper ones. This procedure was adopted for a sample of 683 clusters with BCGs from the SDSS sample. Average images were obtained after masking all

detectable sources (foreground stars and galaxies), centering and scaling; they provide average properties of the diffuse optical light. The results for the integrated light fractions within 500 kpc cluster radius are BCG:ICL:galaxies = 21.9:10.9:67.2, with a robust estimate of the fraction (ICL+BCG)/(total light) being about 30%. The color of ICL is similar to the color of galaxy light in the cluster, and the radial profile of the ICL is more centrally concentrated than that of the light in cluster galaxies. References: Zibetti et al. (2005), Pierini et al. (2008).

2.3.3. *The diffuse intergalactic light in intermediate redshift clusters : RXJ0054-2823 - J. Melnick*

An “S”- shaped arc, bluer than the cD galaxies and the ICL, has been detected in the intermediate redshift cluster RXJ0054-2823 using the consecutive differential image technique. There are no emission lines associated with this arc and its redshift is consistent with the cluster redshift, i.e. it is not a lensed background galaxy image. The arc is probably formed by two spirals caught in the act of being tidally crunched by the three giant galaxies in the cluster center. References: Melnick et al. (1999), Faure et al. (2007).

3. Kinematics of Intracluster stars - individual stars and absorption line spectroscopy

3.1. *Properties of intracluster starlight - A. Zabludoff*

The intracluster stars are hard to count: yet, they are significant in the understanding of the origin of baryon vs. dark matter distributions and the enrichment of stars and gas in clusters. ICL is here detected in terms of an additional de Vaucouleurs profile required to fit the surface brightness profile of the central galaxy at large radii. A two-dimensional fit with a single profile is often poor at large radii, and fails both for the ellipticity and position angle profiles. The BCG and the outer component are aligned within 10 deg about 40% of the time; in the rest of the cases the misalignment is large. The extrapolated light of the outer component dominates the total and its color is similar to that of an old population. The increase of the velocity dispersion measured in several clusters suggests that it responds to the cluster potential. References: Kelson et al. (2002), Zaritsky et al. (2006), Gonzalez et al. (2007).

3.2. *Intracluster planetary nebulae and globular clusters*

Discrete objects like planetary nebulae (PNe) are excellent tracers for measuring the line-of-sight (LOS) kinematics of intracluster stars: PNe occur during the final phase of solar type stars, their number density distribution follows light, and their nebular shell re-emits more than 10% of the UV light from the stellar core in one optical emission line, [OIII]5007Å. This bright emission line makes it possible to detect and measure the velocity of such stars even in regions where the total surface brightness is too faint for absorption line spectroscopy. By surveying large areas in clusters, a suitable number of PNe can be detected and mean radial velocities and velocity dispersions can be determined.

Such investigations have been carried out in a number of nearby clusters and this section covers the recent observational results in this field. Similar studies are possible using globular clusters, assuming these also trace the distribution of stars. Studies based on globular clusters are reported in Section 4.

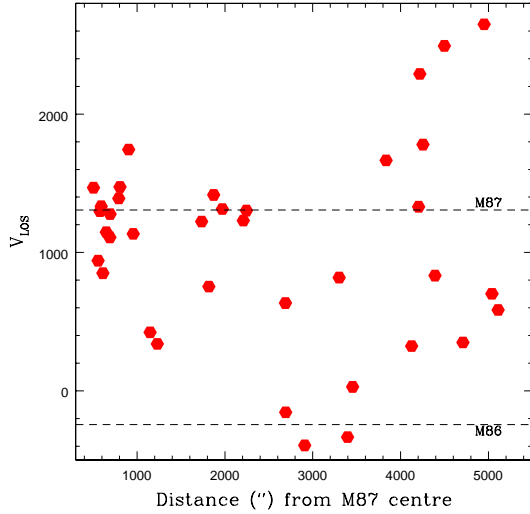


Figure 2. Distribution of line-of-sight velocity versus projected distance from the center of M87 for all spectroscopically confirmed PNs in the 6 FLAMES fields in the Virgo cluster core. From Doherty et al. (2009).

3.2.1. Kinematics of diffuse light in the Virgo cluster core from planetary Nebulae - M. Arnaboldi

The kinematics of the ICL in the Virgo cluster was studied using the PNe identified in narrow band surveys. The FLAMES spectrograph at the VLT was used for the spectroscopic campaign, with a total of 6 VLT-Flames pointings observed. From the positions and velocities of the detected PNe a projected phase-space diagram was built which illustrates the different dynamical components along the LOS in the Virgo cluster core, see Fig. 2: these are the extended halo of M87 and the ICL component. Within $R < 3600'' = 260$ kpc from M87, the ICL component is all at negative velocities relative to M87, and it is not phase-mixed. Part of this component is at velocities consistent with the idea that light of the M86 sub-group is being tidally stripped by the more massive M87 component, while the two galaxies approach each other along the LOS. By contrast, in a more distant field at $R = 4500''$, the full velocity width of the Virgo cluster is seen. References: Arnaboldi et al. (1996, 2004), Doherty et al. (2009).

3.2.2. Dynamics of cluster cores and brightest galaxies from planetary nebulae velocities - O. Gerhard

Numerical simulations predict that isolated galaxies acquire extended radially anisotropic halos built from accretion of smaller galaxies; the level of predicted anisotropy is consistent with results from a few nearby ellipticals studied so far. In simulated BCG galaxies, additional high-velocity components from disrupted or stripped galaxies may be superposed on the central galaxy. Observationally, the outer halos of the BCGs at the centers of the Fornax, Virgo, Coma and Hydra I clusters are in fact harbouring substructure associated with disrupted satellites. In all cases the data indicate that galaxy halos and ICL are discrete components; the former do not blend continuously into the latter, and there is no evidence for a continuous increase of the galaxy velocity dispersion to cluster values, but rather a colder BCG halo is superposed with a hotter ICL component

at radially decreasing surface brightness ratio. The evidence for merging (in Coma) and accretion/disruption indicates that the build-up of the BCG and ICL is an on-going and long-lasting process. References: Gerhard et al. (2007), Murante et al. (2007), de Lorenzi et al. (2009).

3.2.3. *The kinematics of intracluster planetary nebulae in the Hydra I cluster - G. Ventimiglia*

The Hydra I cluster is a relaxed cluster from its regular X-ray emission, in the Southern hemisphere at 50 Mpc distance. At this distance, even the emission line flux from the brightest PN is only 8×10^{-18} erg s $^{-1}$ cm $^{-2}$; thus to detect these objects the sky noise must be substantially reduced. This can be achieved with the “multi slit imaging spectroscopy” technique (MSIS), a blind technique which combines the use of a mask with parallel slits, a narrow band filter and a grism, yielding spectra a few tens of Å wide for all emission objects which lie behind the slits. With FORS2 and the VLT, in a 6.8 arcmin 2 squared field centred on NGC 3311, a total of 82 emission line objects were identified: 56 are PN candidates and 26 background galaxies. The m_{5007} magnitudes are consistent with a PN population at 50 Mpc distance, and the PN LOSVD shows three velocity components: a main cluster component at the cluster’s redshift and expected $\sigma = 600$ km s $^{-1}$, plus two discrete colder components at a bluer (1800 km s $^{-1}$) and a redder (5000 km s $^{-1}$) velocity, providing evidence for unmixed components in the NGC 3311 halo. References: Gerhard et al. (2005), Arnaboldi et al. (2007), Ventimiglia et al. (2008).

3.2.4. *Planetary nebulae in NGC 1399: the kinematics of a cD halo - E. McNeil*

A counter dispersed imaging spectroscopy study with a mosaic of 5 pointings has been carried out, covering the bright central parts and extended halo of the Fornax cD galaxy NGC 1399. These observations deliver a sample of PN positions, measured magnitudes and velocities, which can be used to construct a 2D velocity field and study the kinematics of the extended halo. In this sample, 146 PNe associated with NGC 1399 are detected, 23 PNe associated with NGC 1404, and 6 unassigned. From the projected phase space diagram v_{LOS} vs. radius, 12 PNe are identified which are associated with a new low velocity component superposed onto NGC 1399. The velocity dispersion profile at large radii in NGC 1399 is consistent with a flat profile at 250 km s $^{-1}$; the rise to Fornax cluster dispersion is not yet reached at these radii. References: Arnaboldi et al. (1994), Saglia et al. (2000), Mc Neil et al. (in preparation).

4. Intracluster stellar populations - [Fe/H] and age distribution

4.1. *Planetary nebulae as tracers of stellar populations - R. Ciardullo*

PNe can be powerful probes of the chemical history of stellar populations. However, a full analysis of the α -element metallicity distribution function based on the nebular line ratios and the detection of the temperature-sensitive [OIII]4363Å line is not yet feasible for intracluster studies. Still it is possible to search for evidence of a metal-rich intracluster population with PN deep spectroscopy, but such spectroscopic data must reach ~ 20 times fainter than [OIII] $\lambda 5007$ fluxes, and the next generation of telescope may be crucial for this. PN counts (normalized to underlying luminosity) do probe the stellar population, but we need a better theoretical understanding of how these objects come to form. If the blue straggler hypothesis is correct, then we may soon be able to use PNe to measure/constrain the age of an old stellar population. References: Feldmeier et al. (2004b), Ciardullo et al. (2005), Buzzoni et al. (2006).

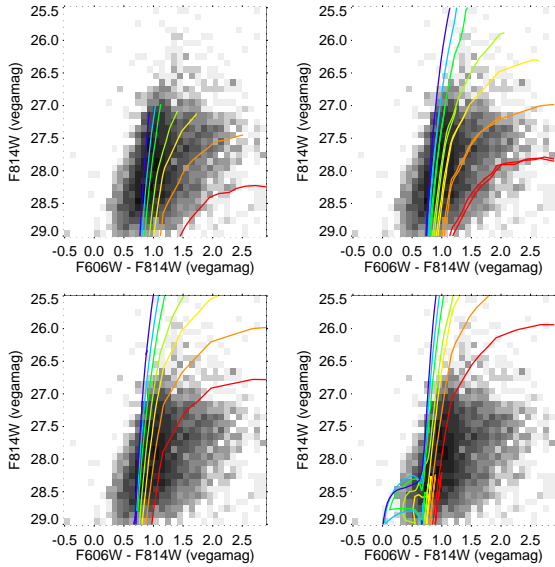


Figure 3. Results from the VICS project. Observed colour magnitude diagram of the VICS Virgo field, with a subset of the Girardi et al. (2002) isochrones for the HST ACS filters superposed. In each panel, the isochrones represent stars with metallicities of $Z = 0.0001, 0.0004, 0.001, 0.0025, 0.004, 0.008$, and 0.019 , with redder isochrones corresponding to higher values of Z . Each panel displays a different age: $\log(\text{age}) = 10.1$ (upper left; the contribution of the AGB was removed from these isochrones), 9.65 (upper right), 9.0 (lower left), and 8.5 (lower right). From Williams et al. (2007).

4.2. The intracluster red giant star population in the Virgo cluster - P. Durrell

Intracluster red giant branch (RGB) stars are the most numerous visible component of ICL; with RGB stars, we can determine the metallicities and constrain the ages of the stellar population(s) (latter with AGB) and relate these to the galactic origin of diffuse stellar light. The IC-RGB stars in Virgo can be studied only with very deep imaging, e.g., HST, which implies a limited field of view. The study of the VICS field yielded over 5000 IC-RGB stars whose color magnitude diagram shows a clear RGB populated by ~ 5300 IC-RGB and AGB stars, above a small background contamination, see Fig. 3. These intracluster RGB stars are mostly old and metal-poor in the surveyed field, and they are not well-mixed even on small scales. These results are consistent with stripping of stars from a wide variety of galaxies, from dwarfs to the outer regions of ellipticals and spirals. References: Durrell et al. (2002), Williams et al. (2007).

4.3. Intracluster globular clusters and ultra-compact dwarfs - M. Hilker

Galaxy clusters are the places of highest galaxy density in the local universe, their cores are dominated by giant ellipticals with an extended surface brightness envelope (cD halo). Globular clusters are excellent tracers of diffuse stellar populations due to their abundant numbers and brightness. The central cluster galaxies possess extremely rich globular cluster systems ($\sim 10,000$ GCs) with an equal amount of red (metal-rich) and blue (metal-poor) GCs. The predominant GC population in intra-cluster regions are the blue (metal-poor) GCs which can be found out to large cluster-centric radii. Also very massive star clusters/ultra-compact dwarf galaxies (UCDs, $10^6 - 10^8 M_\odot$) are found in the intra-cluster space. Some of these might have had their origin as nuclei of now disrupted

dwarf galaxies. References: Richtler et al. (2004), Schuberth et al. (2009), Misgeld et al. (2009).

4.4. *Intergalactic globular clusters - M. West*

Numerical simulations suggest large populations of intergalactic globulars could exist in rich galaxy clusters. There is evidence of wide-spread galaxy stripping and destruction. The Jeans mass at recombination was $\sim 10^5 - 10^6$ solar masses, and therefore globular clusters could form anywhere the mass density was high enough. The Abell cluster 1185 provides clear evidence for IC GCs found near the peak of the Xray emission which does not coincide with the center of the cluster galaxy number density distribution. The deep ACS image at this position shows an excess of point-like sources with respect to the control fields. A large population of IGCs ($\sim 50,000$ GCs) is observed in Coma, while the Virgo cluster has a small population. References: Jordan et al. (2009), Takamiya et al. (2009).

4.5. *Stellar kinematics and line strength indices in BCG halos - L. Coccato*

The bright galaxies at the centers of galaxy clusters often have extended halos whose presence is considered to be the result of the co-evolution of the central galaxy and its cluster environment. Information on the time of formation of the different components comes from the study of their stellar populations, which may provide both age and metallicity profiles. Long slit absorption line spectroscopy of the two BCG galaxies in the Coma cluster, NGC 4889 and NGC 4874, was performed at the Subaru 8 m telescope, with the FOCAS spectrograph. The integrated light spectra had adequate S/N so that absorption line indices for NGC 4889 could be determined out to 65 kpc. The results show that within $1.2R_e$ the stars of NGC 4889 must have formed over a very short time scale (< 1 Gyr), with little subsequent merging, as shown by the large α -enhancement and the measured steep metallicity gradient. The stars in the halo were formed on a longer time scale, as shown by the lower α/Fe values. This is compatible with formation in smaller systems which were subsequently accreted onto the halo of the BCG. References: Coccato et al. (in preparation).

5. Cosmological simulations of cluster and group formation/Origin of diffuse light

5.1. *Cluster and group formation in Λ CDM - S. White*

Starting from cosmological Λ CDM initial conditions, numerical simulations of the formation of large scale structure can now predict and reproduce the average mass profiles and properties of clusters and groups in the mass range $10^{12} M_\odot$ - $10^{15} M_\odot$. Table 1 shows some parameters for the Millenium-II simulation. Together with semi-analytic models the simulations can be used to study the stellar mass function of galaxies in groups and clusters down to $10^7 M_\odot$, which is found to have similar shape as in the field except for the BCGs. Assuming the ICL is due to tidally stripped and disrupted galaxies, based on galaxy orbits and sizes and stripping of the DM halo, the simulations can be used to predict the fraction of cluster light in the ICL. Considerable scatter in the fractions of ICL relative to ICL + BCG (within $\sim 40 \pm 30\%$) and relative to the total cluster light (within $\sim 15 \pm 15\%$) is found, due to variations in assembly/stripping history. References: Springel, Frenk and White (2006), Hilbert and White (2009), Guo et al. (2009).

Table 1. The Millennium-II simulation: particle number and mass, size of simulated volume, resolution (softening), and fraction of particles in lumps at $z=0$.

N_{part}	m_{part} $h^{-1}M_{\odot}$	L $h^{-1}Mpc$	ϵ $h^{-1}kpc$	$F_{halo}(z=0)$
2160^3	6.9×10^6	100	1	0.60

5.2. Galaxy evolution in clusters and groups - L. Mayer

The physical mechanisms for galaxy transformation at work in cluster environments can be grouped into two categories: tidal interactions, and ICM-galaxy interactions. The latter can take place in several flavours: ram pressure stripping of cold ISM in disks; triggered star formation and strangulation; stripping of gaseous halos around galaxies. These processes help to build up the morphology density relation, i.e., that early-type galaxies (E,S0,dE,dS0) dominate in cluster cores, and explain the high number density of early-type dwarf galaxies at the centers of nearby groups and clusters, the HI deficiency of galaxies in cluster centers, and the steepening of the faint end of the luminosity function relative to the field. These transformations were studied with simulations replacing dark halos in dark matter only simulations at the time of infall with multi-component late type galaxy models. Cosmological simulations of groups show that mergers drive morphology towards elliptical systems, and that at large $R > 5R_e$ a diffuse stellar halo or intragroup light component is formed which may comprise $\sim 20\%$ of the group light. References: Mastropietro et al. (2005), Mayer et al. (2006).

5.3. Galaxy properties in clusters: dependence on the environment - H. Muriel

This work investigated the dependence of several galaxy properties on the environment and cluster identification techniques. Clusters of galaxies were selected from two catalogues based on the SDSS: the ROSAT-SDSS Galaxy Cluster Survey, and the MaxBCG Catalogue. Galaxies in X-ray and MaxBCG selected clusters show similar size-luminosity relations. The Faber-Jackson relation for early-type galaxies in clusters is also the same for X-ray selected and MaxBCG clusters. BCGs, non-BCG-early type galaxies in clusters and field early-type galaxies show different size-luminosity relations and have different dynamical properties. Using several criteria to classify galaxies into morphological types, the well known morphological segregation can be reproduced. These results can be related to the different processes that affect the evolution of galaxies in various environments. References: Coenda and Muriel (2009).

5.4. Diffuse stellar component in cosmological simulations - K. Dolag

Cosmological hydro-dynamical simulations of zoomed-in clusters have been performed with up to 4×10^6 particles in R_{vir} , radiative cooling/heating by UV background (quasars), a sub-grid two-phase model for star-formation, thermal and kinetic feedback by supernovae; and evolving stellar populations (SNIa/SNII). In these simulations it is possible to separate galaxies, the BCG, and the ICL, using substructure finding algorithms and the full phase-space information of the stellar particles. The ICL surface brightness profile is found to be steeper than the average galaxy light from cluster galaxies averaged in annuli. From the analysis of the merger trees in these cluster simulations, no preferred formation time for the ICL is found, and because it is cumulative, the largest contribution is released at $z < 1$. Most of the ICL comes from merging processes, either with the BCG or prior to infall into the cluster; other contributions are significant only outside $0.5R_{vir}$. Mergers liberate up to 30% of stars in both galaxies. Related with the finite resolution

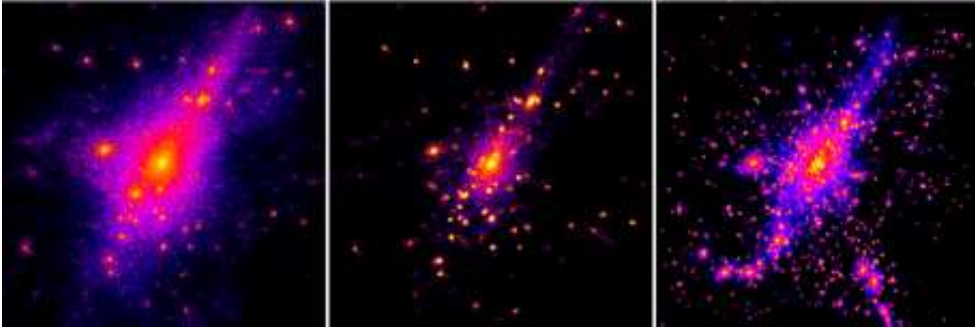


Figure 4. The distribution of the dark matter (DM, left), and of the stars (center), for a simulated cluster, and the distribution of stars in a high-resolution re-simulation of the same cluster (right), all at redshift $z = 0$. The frames are $6h^{-1}$ Mpc on a side, corresponding to $\approx 2R_{\text{vir}}$. They show density maps generated with different logarithmic colour scales for DM and stars. The galaxy and diffuse components in each panel can clearly be seen. From Murante et al. (2007).

of the simulations, a sizable contribution comes from dissolved galaxies, but whether this is a robust estimate cannot be firmly established at this stage. References: Murante et al. (2004, 2007), Dolag et al. (2009).

5.5. *Extended ionized and molecular gas emission in galaxy clusters - R. Oonk*

New, deep integral-field spectroscopy and imaging of the extended molecular and ionized gas distributions within the central regions of several galaxy clusters is presented, obtained with the VLT and HST. These observations show the existence of gas surrounding the BCG, extending at least up to 20 kpc from the nucleus. The H2 to HII line ratios are very high and are different from typical AGN and starburst ratios. To date no single source of excitation has successfully explained all line ratios over the entirety of the observed gas distribution. Various line diagnostics are used to constrain the properties of the observed gas and discuss its origin and fate. The question is open whether this is a birthplace of some of the stars in the ICL. References: van Weeren et al. (2009).

6. Summary of the discussion

The discussion at the end of the workshop was introduced by M. Arnaboldi with a quote from Uson et al. (1991): "Whether this diffuse light is called the cD envelope or diffuse intergalactic light is a matter of semantics; it is a diffuse component which is distributed with elliptical symmetry about the center of the cluster potential". A lively discussion then developed about the progress achieved since the time of this paper, with the main contributors being M. Arnaboldi, R. Ciardullo, P. Durrell, J. Feldmeier, C. Mihos, S. White, and A. Zabludoff. In the following, we list the main topics of discussion, and the specific conclusions and open issues that emerged for each of them. Because this list reflects only our understanding of what was being said, we apologize in advance for any errors or omissions.

ENVELOPE OF BRIGHTEST CLUSTER GALAXY VERSUS ICL:

- Sometimes the ICL is not aligned with BCG isophotes, so from this fact alone one would conclude that cD halo and ICL are different components.
- In some clusters like Coma and Abell 1185 an extended ICL component embeds

more than one BCG. In Abell 545, a bright diffuse light component is seen with several galaxies embedded, but no cD. The ICL must therefore be a component distinct from a galaxy halo.

- There is kinematic evidence from PN and GC velocity distributions in the centers of nearby galaxy clusters that ICL and BCG halos are distinct physical components.
- There is a clear need for more spectroscopic data, to disentangle the contribution of halo and cluster component.

HOW TO MEASURE THE FRACTION OF ICL?

- The fraction of ICL is an observationally ill-defined quantity, either depending on arbitrary surface brightness thresholds in photometric studies, or lacking the full phase-space information to ascertain whether a star is bound to the central galaxy or not. A comparison with simulations is therefore difficult.
- Thus it would be useful if simulations were analysed to produce surface brightness maps. This would facilitate the comparison with wide field photometry measurements. One would then adopt a surface brightness threshold and make comparisons between the observed and simulated ICL plus BCG envelope fractions.
- A useful measurement to quantify the dynamical status of the ICL would be the fraction of homogenous versus irregular light or, more generally, the power spectrum over spatial scales.

TO WHAT REDSHIFT CAN WE GO WITH ICL STUDIES?

- Since much of the merging of massive galaxies occurs from $z=1$ to $z=0$, it would be interesting to reach $z=0.3$ with studies of ICL morphology, photometry and kinematics. Redshifts higher than $z=0.3$ may be out of reach because of the strong surface brightness dimming effect scaling $\propto (1+z)^{-4}$ with redshift z .
- The deep data sets obtained in weak lensing surveys may be useful for the determination of ICL morphology and photometry in intermediate redshift clusters.

METALLICITY AND COLOUR AS OBSERVATIONAL CONSTRAINTS ON HOW ICL IS MADE:

- In the VICS field in Virgo the intracluster stars are mostly old and mostly metal poor with a large metallicity spread; this is consistent with stripping of stars from a wide variety of galaxies, including the halos (but not the inner regions) of ellipticals.
- Most of the ICL in moderate redshift clusters, that is the more nearly homogeneous part, has the same color as the early-type galaxies in the cluster core.
- Blue colors are measured most often for elongated stream-like features.
- It would be very important to use cosmological simulations to predict the metallicity distribution and colours of ICL stars, and to compare this with present data.

RESULTS FROM SIMULATIONS ON THE ORIGIN OF ICL:

- In cosmological simulations of cluster formation, most of the ICL comes from the halos of evolved galaxies. Does this need to be reconciled with the results from higher-resolution simulations of galaxy evolution in dense environments?
- The importance of groups in generating ICL must be emphasized, through creating

loosely bound stars in group interactions (“pre-processing”) which are later unbound by the gravitational potential of the cluster into which they fall.

- Groups are generally important because of their environmental effects on galaxy evolution, and thus indirectly, the ICL.

THE HIGH-MASS END OF THE GALAXY LUMINOSITY FUNCTION:

- Is there still a problem caused by the evolution of the high mass end of the galaxy mass function from redshift $z=1$ to $z=0$?
- With semi-analytical models one can adjust the parameters for the AGN feedback, and recover agreement with observations. In the case of hydro-dynamical simulations, there is still a problem, and the dispersion of stars in the cluster volume as ICL would help.

FUTURE PROSPECTS:

- Currently we see a lot of new data on intracluster globular clusters from the Virgo/Coma legacy surveys. It will require lots of spectroscopic time to do the kinematic follow-up observations but the result will definitely be worth it.
- Resolved stellar populations in the Virgo and Fornax cluster ICL are obvious targets for the E-ELT, JWST, because crowding is not a problem at these low surface brightness levels.

CONCLUDING REMARK: Jorge Melnick summarized the meeting by stating that he was very pleased to see the subject of ICL to be active and strong, with extensive developments in deep surface brightness measurements, kinematics, stellar population studies, and comparisons with cosmological simulations. A very interesting meeting, much new science, and hope for more in Beijing!

7. Poster Papers

- ABS N. 123: Eduardo Cypriano et al. - Shrinking of cluster ellipticals: a tidal stripping explanation and implications for the intracluster light
- ABS N. 210: Marcelo Bryrro Ribeiro - Differential density statistics of the galaxy distribution and the luminosity function
- ABS N.450: Margarita Rosado et al. - Diffuse light in the Seyfert’s Sextet
- ABS N.855: Tiberio Borges Vale et al. - Environmental effects on the structure of galaxy discs
- ABS N.992: Cristina Furlanetto et al. - Detection of gravitational arcs in galaxy clusters
- ABS N.1877: Walter Augusto Santos et al. - Photometric redshifts for SDSS galaxies using locally weighted regression.
- ABS N.1951: Julio Saucedo et al. - A study of the galaxy population in the region of A1781
- ABS N. 1962: Yasuhiro Hashimoto et al. - Multi-wavelength study of cluster morphology and its implications on the scaling relations, mass estimate, large scale structure, and evolution of galaxies.
- ABS N. 2076: Steven Michael Crawford et al. - The evolution of cluster galaxies and the diffuse intracluster light

- ABS N. 2341: Simon Nicholas Kemp et al. - From cDs to diffuse structures: faint light in galaxies using Schmidt and CCD data
- ABS N. 2728: Mangala Sharma et al. - Tracing galaxy group dynamical histories through diffuse intergalactic light.
- ABS N. 2947: Sadanori Okamura et al. - Observation of intracluster diffuse light in the Coma cluster
- ABS N. 2990: Roderik Overzier - Examining the Spiderweb: forming a BCG and its intracluster light at $z=2$
- ABS N. 3002: Nieves Castro-Rodriguez et al. - Intracluster light in the Virgo cluster: large scale distribution.

Acknowledgements

We would like to acknowledge the support from the IAU, and the hard work and enthusiasm of the participants, which made this IAU Joint Discussion #2 on Diffuse Light in Galaxy Clusters both possible and stimulating.

References

- Adami, C., Biviano, A., Durret, F., & Mazure, A. 2005a, *A&A*, 443, 17
- Adami, C., et al. 2005b, *A&A*, 429, 39
- Arnaboldi, M., Freeman, K. C., Hui, X., Capaccioli, M., & Ford, H. 1994, *The Messenger*, 76, 40
- Arnaboldi, M., et al. 1996, *ApJ*, 472, 145
- Arnaboldi, M., Gerhard, O., Aguerri, J. A. L., Freeman, K. C., Napolitano, N. R., Okamura, S., & Yasuda, N. 2004, *ApJ*, 614, L33
- Arnaboldi, M., Gerhard, O., Okamura, S., Kashikawa, N., Yasuda, N., & Freeman, K. C. 2007, *PASJ*, 59, 419
- Buzzoni, A., Arnaboldi, M., & Corradi, R. L. M. 2006, *MNRAS*, 368, 877
- Ciardullo, R., Sigurdsson, S., Feldmeier, J. J., & Jacoby, G. H. 2005, *ApJ*, 629, 499
- Coenda, V., & Muriel, H. 2009, *A&A*, 504, 347
- Da Rocha, C., Ziegler, B. L., & Mendes de Oliveira, C. 2008, *MNRAS*, 388, 1433
- de Lorenzi, F., et al. 2009, *MNRAS*, 395, 76
- de Mello, D. F., Torres-Flores, S., & Mendes de Oliveira, C. 2008, *AJ*, 135, 319
- Doherty, M., et al. 2009, *A&A*, 502, 771
- Dolag, K., Murante, G., & Borgani, S. 2009, arXiv:0911.1129
- Durrell, P. R., Ciardullo, R., Feldmeier, J. J., Jacoby, G. H., & Sigurdsson, S. 2002, *ApJ*, 570, 119
- Faure, C., Giraud, E., Melnick, J., Quintana, H., Selman, F., & Wambsganss, J. 2007, *A&A*, 463, 833
- Feldmeier, J. J., Mihos, J. C., Morrison, H. L., Harding, P., Kaib, N., & Dubinski, J. 2004a, *ApJ*, 609, 617
- Feldmeier, J. J., Ciardullo, R., Jacoby, G. H., & Durrell, P. R. 2004b, *ApJ*, 615, 196
- Gerhard, O., Arnaboldi, M., Freeman, K. C., et al. 2005, *ApJ*, 621, L93
- Gerhard, O., Arnaboldi, M., Freeman, K. C., Okamura, S., Kashikawa, N., & Yasuda, N. 2007, *A&A*, 468, 815
- Girardi, L., Bertelli, G., Bressan, A., Chiosi, C., Groenewegen, M. A. T., Marigo, P., Salasnich, B., & Weiss, A. 2002, *A&A*, 391, 195
- Gonzalez, A. H., Zaritsky, D., & Zabludoff, A. I. 2007, *ApJ*, 666, 147
- Guo, Q., White, S., Li, C., & Boylan-Kolchin, M. 2009, arXiv:0909.4305
- Hilbert, S., & White, S. D. M. 2009, arXiv:0907.4371
- Jordán, A., et al. 2009, *ApJS*, 180, 54
- Kelson, D. D., Zabludoff, A. I., Williams, K. A., et al. 2002, *ApJ*, 576, 720

- Krick, J. E., & Bernstein, R. A. 2007, *AJ*, 134, 466
- Mayer, L., Mastropietro, C., Wadsley, J., Stadel, J., & Moore, B. 2006, *MNRAS*, 369, 1021
- Mastropietro, C., Moore, B., Mayer, L., Debattista, V. P., Piffaretti, R., & Stadel, J. 2005, *MNRAS*, 364, 607
- Melnick, J., Selman, F., & Quintana, H. 1999, *PASP*, 111, 1444
- Mihos, J. C., Harding, P., Feldmeier, J., & Morrison, H. 2005, *ApJ*, 631, L41
- Mihos, J. C., Janowiecki, S., Feldmeier, J. J., Harding, P., & Morrison, H. 2009, *ApJ*, 698, 1879
- Misgeld, I., Hilker, M., & Mieske, S. 2009, *A&A*, 496, 683
- Murante, G., et al. 2004, *ApJ*, 607, L83
- Murante, G., Giovalli, M., Gerhard, O., Arnaboldi, M., Borgani, S., & Dolag, K. 2007, *MNRAS*, 377, 377
- Pierini, D., Zibetti, S., Braglia, F., Böhringer, H., Finoguenov, A., Lynam, P. D., & Zhang, Y.-Y. 2008, *A&A*, 483, 727
- Richtler, T., Dirsch, B., Gebhardt, K., et al. 2004, *AJ*, 127, 2094
- Saglia, R. P., Kronawitter, A., Gerhard, O., & Bender, R. 2000, *AJ*, 119, 153
- Salinas, R., Richtler, T., Romanowsky, A. J., West, M. J., & Schuberth, Y. 2007, *A&A*, 475, 507
- Schuberth, Y., Richtler, T., Hilker, M., Dirsch, B., Bassino, L. P., Romanowsky, A. J., & Infante, L. 2009, arXiv:0911.0420
- Springel, V., Frenk, C. S., & White, S. D. M. 2006, *Nature*, 440, 1137
- Takamiya, M., West, M., Côté, P., Jordán, A., Peng, E., & Ferrarese, L. 2009, *Globular Clusters - Guides to Galaxies*, 361
- Thuan, T.H., Kormendy, J. 1977, *PASP*, 89, 466
- Torres-Flores, S., Mendes de Oliveira, C., de Mello, D. F., Amram, P., Plana, H., Epinat, B., & Iglesias-Páramo, J. 2009, *A&A*, 507, 723
- Uson, J. M., Boughn, S. P., & Kuhn, J. R. 1991, *ApJ*, 369, 46
- van Weeren, R. J., Intema, H. T., Oonk, J. B. R., Rottgering, H. J. A., & Clarke, T. E. 2009, arXiv:0910.4967
- Ventimiglia, G., Arnaboldi, M., & Gerhard, O. 2008, *Astronomische Nachrichten*, 329, 1057
- Zaritsky, D., Gonzalez, A. H., & Zabludoff, A. I. 2006, *ApJ*, 638, 725
- Zibetti, S., White, S. D. M., Schneider, D. P., & Brinkmann, J. 2005, *MNRAS*, 358, 949
- Williams, B. F., et al. 2007, *ApJ*, 656, 756

